New Journal of Physics
The open access journal for physics

Stabilization of photon collapse and revival dynamics by a non-Markovian phonon bath

Alexander Carmele[1,2,3], **Andreas Knorr**[1] **and Frank Milde**[1]

[1] Institut für Theoretische Physik, Nichtlineare Optik und Quantenelektronik, Technische Universität Berlin, Hardenbergstraße 36, EW 7-1, D-10623 Berlin, Germany

[2] Institute for Quantum Optics and Quantum Information, Austrian Academy of Sciences, Technikerstrasse 25, 6020 Innsbruck, Austria

E-mail: alex@itp.physik.tu-berlin.de

New Journal of Physics **15** (2013) 105024 (13pp)
Received 2 August 2013
Published 23 October 2013
Online at http://www.njp.org/
doi:10.1088/1367-2630/15/10/105024

Abstract. Solid state-based light emitters such as semiconductor quantum dots (QDs) have been demonstrated to be versatile candidates to study the fundamentals of light–matter interaction. In contrast to optics with isolated atomic systems, in the solid-state dissipative processes are induced by the inherent coupling to the environment and are typically perceived as a major obstacle toward stable performances in experiments and applications. In this theoretical model study we show that this is not necessarily the case. In fact, in certain parameter regimes, the memory of the solid-state environment can enhance coherent quantum optical effects. In particular, we demonstrate that the non-Markovian coupling to an incoherent phonon bath can exhibit a stabilizing effect on the coherent QD cavity-quantum electrodynamics by inhibiting irregular oscillations and allowing for regular collapse and revival patterns. For self-assembled GaAs/InAs QDs at low photon numbers we predict dynamics that deviate dramatically from the well-known atomic Jaynes–Cummings model. Even if the required sample parameters are not yet available in recent experimental achievements, we believe our proposal opens the way to a systematic and deliberate design of photon quantum effects via specifically engineered solid-state environments.

[3] Author to whom any correspondence should be addressed.

Semiconductor quantum dots (QDs), coupled to a photonic cavity, exhibit signatures of strong coupling [1–8] when the electron–photon interaction outrivals the combined dipole decay rate and cavity loss. In contrast to fundamental atom–photon interfaces [9], a key factor to the understanding of observed phenomena in the semiconductor cavity-quantum electrodynamics (cQED) regime is the interaction of electrons with the QD host material. The inherent many-body properties of a solid-state, in particular the electron–phonon interaction, lead to often undesired decoherence, where the superposition of otherwise distinct quantum states becomes lost and information about the system is carried away into the host material surrounding of the embedded QD [10, 11]. In principle, this dephasing mechanism seems to put limits on the prospects of the wide field of semiconductor-based quantum information processing and quantum communication [12]. However, it has been shown that in photosynthetic systems, for example, the quantum-coherent excitation transfer in Fenna–Matthews–Olsen antenna complexes is not only resistant to dephasing [13], but is actually supported by the dephasing processes induced by the thermal fluctuations of the molecule [14, 15]. This sparked a lively debate over its implications for evolutionary biology, energy technologies and quantum information [16].

It is also known that lattice vibrations in semiconductor nano structures can give rise to new effects and dynamics [17] not known in atomic quantum optics, nor in Markovian treatments of the semiconductor environment, e.g. phonon-mediated off-resonant cavity feeding [18–21], formation of phonon-assisted Mollow triplets [22, 23] and temperature-dependent vacuum Rabi splittings seen in cavity emission spectra experimentally [24] and theoretically [25, 26]. Very recently impressive experiments were realized which could steer the transition from Markovian to non-Markovian dynamics and thus the flow of information between an open system and its environment [27].

Expanding on these developments we report on how the non-Markovian coupling to an environment can be counter-intuitively exploited to support coherent quantum optical features. For a solid-state emitter, for illustration described as a semiconductor QD, strongly coupled to a nanocavity, the memory effects of an incoherent bath of harmonic oscillators induce astonishing pattern formations in the coherent collapse and revival phenomenon of the photon dynamics in the cavity. The collapse and revival phenomenon results from the interference of different Rabi frequencies (Jaynes–Cummings ladder contributions) and its fundamentals were investigated both theoretically [28] and experimentally [29, 30]. The presented effect further challenges the widely adopted notion that the environmental coupling, responsible for decoherence, constitutes a substantial drawback that needs to be overcome, in order to build robust solid-state devices using existing semiconductor fabrication technologies. The very same coupling to the surrounding does not destroy, but rather facilitates and stabilizes the otherwise fragile quantum effect of collapse and revival, in particular at the few-photon level, and hence lifts the restriction of the high photon numbers needed in atomic systems to initiate stable collapse and revivals, i.e. for longer times and more cycles.

To provide a basis for discussion of solid-state effects on an equal footing, we start by introducing an approach to a two-level system interacting with (i) photons and (ii) phonons, which encompasses the well-known Jaynes–Cummings model (JCM) and non-Markovian pure dephasing effects, respectively.

For illustration of the effect, we consider an InAs/GaAs self-assembled QD with well separated quantum confined electronic states, i.e. valence (v) and conduction (c) shell. This effective two-level system is embedded in a single-mode photonic cavity and can interact

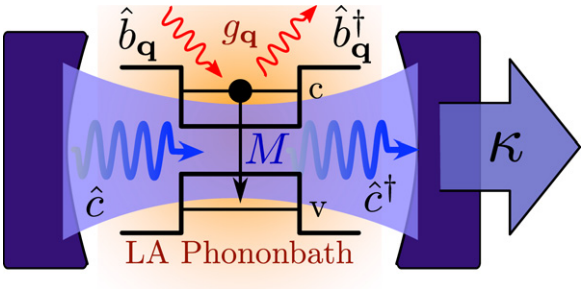

Figure 1. Investigated system. A two-level QD with states v and c in a photonic cavity is coupled to (i) a single cavity mode (blue) via M and (ii) a phonon bath (orange) via $g_{\mathbf{q}}$.

with both, the quantized lattice vibrations of the QD host matrix and the cavity photons, see figure 1. Particularly, we will focus on the interaction of electrons with longitudinal-acoustic (LA) phonons via deformation potential coupling, dominating at low temperatures [31, 32]. The investigation will explore the temporal dynamics of the cavity photon density, since it is experimentally extractable via output coupling [30] or accessible from cavity transmission measurements [33].

The dynamics of the relevant expectation values is derived via the Heisenberg equation

$$-\mathrm{i}\hbar\partial_t \hat{O}(t) = [\hat{H}, \hat{O}]_-. \tag{1}$$

The Hamiltonian of our model includes the free energy of non-interacting electrons, cavity photons and bulk phonons:

$$\hat{H}_0 = \sum_{i}^{\mathrm{v,c}} \hbar\omega_i \hat{a}_i^{\dagger}\hat{a}_i + \hbar\omega_0 \hat{c}^{\dagger}\hat{c} + \sum_{\mathbf{q}} \hbar\omega_{\mathbf{q}} \hat{b}_{\mathbf{q}}^{\dagger}\hat{b}_{\mathbf{q}}^{\dagger} \tag{2}$$

with electron creation (annihilation) operators $\hat{a}_i(\hat{a}_i^{\dagger})$ in shell $i = \mathrm{v}, \mathrm{c}$. Usually, the respective quantized energies $\hbar\omega_i = \varepsilon_i$ are obtained within the effective mass approximation. The frequency of the fundamental cavity mode is ω_0 and $\hat{c}$ $(\hat{c}^{\dagger})$ create (annihilate) a corresponding photon. Phonons with wave vector $\mathbf{q}$ are described by operators $\hat{b}_{\mathbf{q}}$ and $\hat{b}_{\mathbf{q}}^{\dagger}$. Their modes have a linear dispersion $\omega_{\mathbf{q}} = c_{\mathrm{s}} \cdot |\mathbf{q}|$, where c_{s} is the speed of sound. The electron–photon interaction is treated within the dipole and rotating wave approximation [34]

$$\hat{H}_{\mathrm{el-pt}} = -\hbar M(\hat{a}_{\mathrm{v}}^{\dagger}\hat{a}_{\mathrm{c}}\hat{c}^{\dagger} + \hat{a}_{\mathrm{c}}^{\dagger}\hat{a}_{\mathrm{v}}\hat{c}), \tag{3}$$

where we assume an optical coupling strength of $M = 314\,\mu\mathrm{eV}$, which lies within reach of current QD and cavity fabrication technology but is not achieved as of yet. We show a comparison with parameters of a state-of-the-art sample [35] in the end of the paper. Finally, the band diagonal interaction of bulk phonons with the conduction shell QD electrons is given by

$$\hat{H}_{\mathrm{el-pn}} = \sum_{\mathbf{q}} g_{\mathbf{q}} \hat{a}_{\mathrm{c}}^{\dagger}\hat{a}_{\mathrm{c}}(\hat{b}_{\mathbf{q}}^{\dagger} + \hat{b}_{\mathbf{q}}). \tag{4}$$

Note, that the phonon bath is initially in equilibrium with the unexcited QD system. The coupling elements $g_{\mathbf{q}} = g_{\mathbf{q}}^{\mathrm{c}} - g_{\mathbf{q}}^{\mathrm{v}}$ are given in the appendix. In this section, also details are given on how to derive a general set of coupled differential equations, which allows one to determine

the photon dynamics $N(t) = \langle \hat{c}^\dagger \hat{c} \rangle (t)$. The relevant dynamical quantities needed are the photon-assisted ground and excited state density $G^m(t) = \langle \hat{a}_v^\dagger \hat{a}_v \hat{c}^{\dagger m} \hat{c}^m \rangle (t)$ and $X^m(t) = \langle \hat{a}_c^\dagger \hat{a}_c \hat{c}^{\dagger m} \hat{c}^m \rangle (t)$, as well as the photon-assisted polarization $P^m(t) = \langle \hat{a}_v^\dagger \hat{a}_c \hat{c}^{\dagger m+1} \hat{c}^m \rangle (t)$. The number of involved photons is labeled by m. We assume that only one electron is present in the QD and $G^0 + X^0 = 1$ holds. Thus the dynamics of the cavity photons is directly related to the dynamics of the QD and can be obtained via

$$N(t) = G^1(t) + X^1(t). \tag{5}$$

In our simulation we focus on a situation that starts with an inverted QD, i.e. $G^m(t_0) = 0$ and $X^0(t_0) = 1$, and a cavity prepared in a *coherent* photon state with a mean photon number of $N(t_0) = 3.5$ [29]. For now, to explore the undisturbed, basic interaction effects, we assume in our study a lossless cavity $\kappa = 0\,\mu$eV and neglect the radiative coupling of the QD to non-cavity modes $\gamma_{\text{rad}} = 0\,\mu$eV. In the end of this paper we will discuss the influence of these additional loss channels on the dynamics and explore possible parameter regimes. Further details on parameters and initial conditions are found in the appendix.

Before investigating the coupled electron–photon–phonon dynamics and presenting our key results, we will briefly recapitulate the underlying physics in quantum optics with isolated atoms as active systems electron–photon dynamics solely, where the collapse and revival phenomenon is observed but also exhibit restrictions for its observation. Then we show how the solid-state surrounding can reduce certain limitations encountered in isolated atomic systems.

First, we benchmark our model and derive the exact solution of the coherent-state JCM [28] by neglecting the electron–phonon interaction and all other loss channels. For a QD and cavity on resonance figure 2(a) displays the corresponding Rabi oscillations in the mean cavity photon number $N = \langle \hat{c}^\dagger \hat{c} \rangle$. The first few picoseconds show the excitation transfer between the QD and the cavity. Its collapse at 10 ps and subsequent revival within the first 20 ps constitutes the essential feature of the collapse and revival phenomenon, visually supported by the solid gray line. However, due to the low initial photon number of $N(t_0) = 3.5$, the first collapse and revival cycle is not completed and after 30 ps the system drifts into irregular fluctuations, visually supported by the vanishing dashed gray line. For a cavity mode assumed to be on resonance with the fundamental QD transition this behavior can be explained as follows.

For a photon field in a Fock *number state* with *precisely* m photons, the photon density will oscillate between the ground ($N = m$) and excited ($N = m + 1$) with the quantized Rabi frequency $\Omega_m = M\sqrt{m+1}$. In contrast, only a *mean* photon number can be calculated for an initially *coherent field mode*. Here, the typical Jaynes–Cummings solutions of the exact number states are superimposed in an average over the Poissonian distribution $P(m) = \exp(-|\alpha|^2)|\alpha|^{2m}/m!$, which describes a coherent photon state and exhibits a peak at the mean photon number $|\alpha|^2 = N$, see bar charts for $N = 3.5$ and 100 in figure 3, and forms a quantum wave packet having certain reoccurrence times. Consequently, collapse and revivals occur [28]. This behavior relates directly to the quantized nature of the cavity field $[c, c^\dagger] \neq 0$. Typically, only discrete frequencies Ω_m around the mean photon number N interfere, which are initially (at t_0) prepared in a definite state and therefore start a correlated dynamics. With increasing time the superimposed discrete Rabi frequencies exhibit an increasing phase shift and destructive interference is inevitable, see figure 2(a) at around 10 ps. However, this collapse is followed by a revival. The dynamics of this revival phenomenon strongly depends on the mean photon number. Figure 3 shows, that for low mean photon numbers the neighboring Rabi

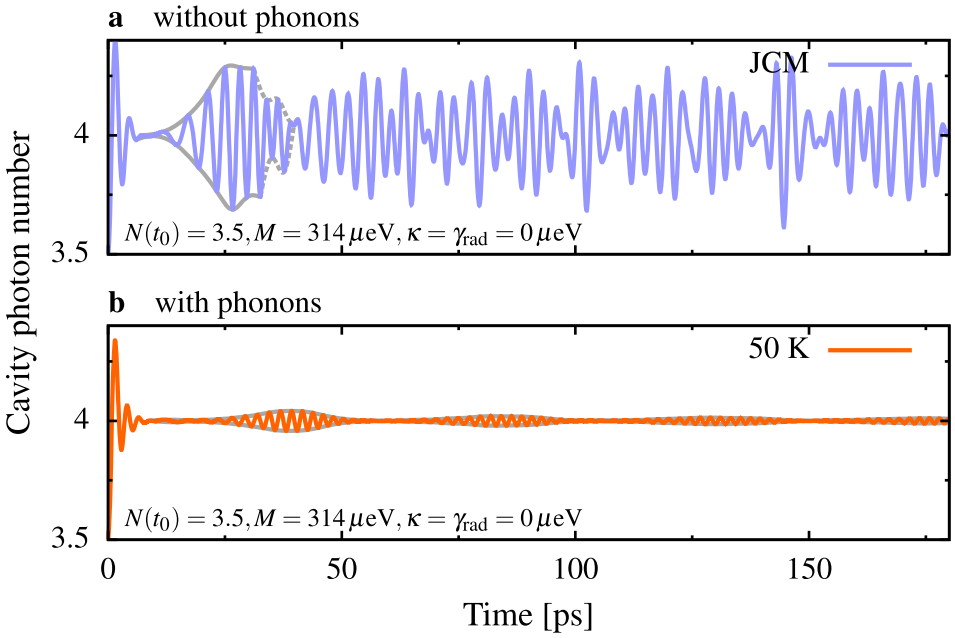

Figure 2. Dynamics of the cavity occupation. (a) Reproduced JCM solution without phonons shows only a single collapse with an incomplete revival. (b) Including phonons with a lattice temperature of 50 K (orange) many-cycle collapse and revivals become possible.

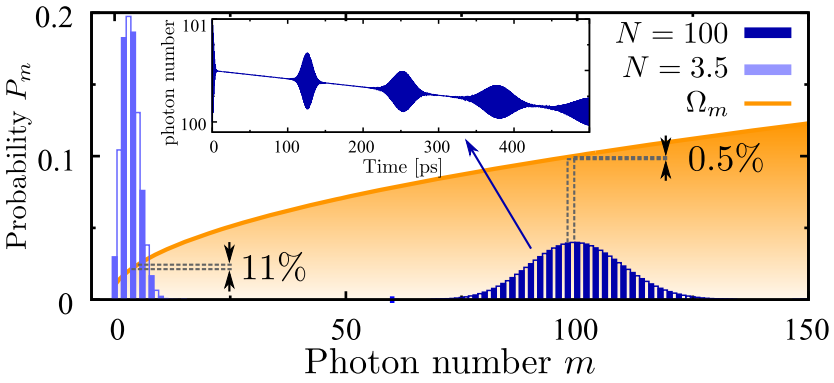

Figure 3. Poissonian distribution P_m to find m photons for different mean photon numbers. The orange line shows the Rabi frequency $\Omega_m = M\sqrt{m+1}$. For $N = 3.5$ (light blue) two neighboring photon states differ in their respective frequency by 11%, while for $N = 100$ (dark blue) only by 0.5%. The inset shows the much more stable collapse and revival for $N = 100$, without phonons.

frequencies Ω_m differ substantially (11%) and their superposition gets out of phase to a point where the initially correlated state is not recovered and the dynamics becomes highly irregular in a quasi-irreversible manner [28], as seen in our simulation in figure 2(a). In contrast, if the mean photon number is high, the impact of spontaneous emission processes is weak ($\sqrt{m+1} \approx \sqrt{m}$), i.e. the phase shift of the superimposed Rabi frequencies is negligible (only 0.5% difference in

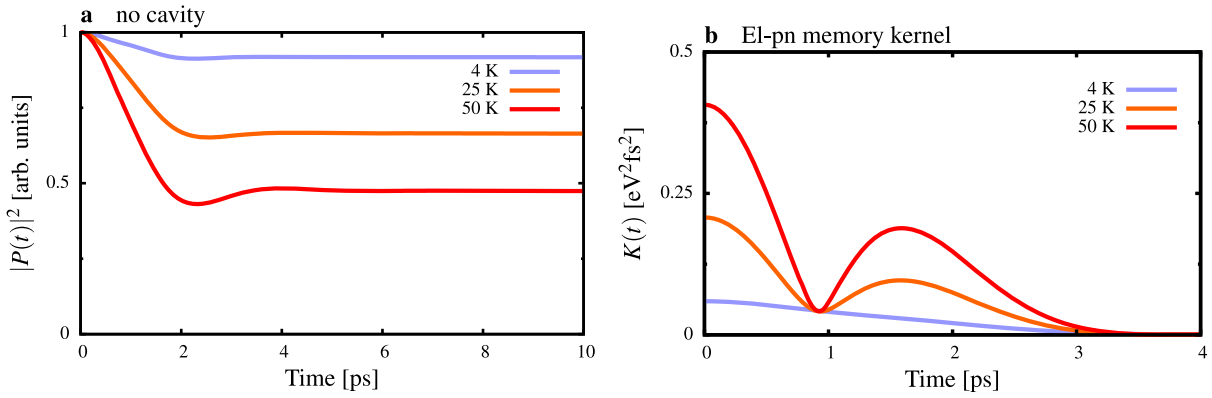

Figure 4. Electron–phonon coupling in QDs. (a) Phonon-induced decay of the QD coherence *in absence* of a cavity and hence without coupling to photons. (b) Absolute value of the corresponding electron–phonon memory kernel. Independent of temperature the kernel vanishes after 4 ps.

Ω_m) and the initially correlated state is recovered. As a result, high photon numbers allow for many regular collapse and revival events in an atomic cQED system, see inset of figure 3. [4]

Now, we turn to the specifics of the light–matter coupling in a solid-state environment inducing electron–phonon interaction and show that high photon numbers are *not necessarily required* to see many collapse and revival events. When including phonons, the photon density shows a strongly modified time evolution, see figure 2(b). Remarkably, the coupling to the phonon bath facilitates regular coherent interference signatures. Depending on the temperature, collapse and revivals survive for much longer times, e.g. for 50 K over 150 ps before fading out.

The counter-intuitive behavior of an incoherent bath of phonons supporting regular coherent features and suppressing seemingly random oscillations can be understood by investigating in detail the coherent polarization P^m of the coupled electron–photon–phonon system, which drives the dynamics of X^m and vice versa.

As an instructive example, consider a simpler case of a QD that interacts solely with its host material and *not* with the quantum light field, first. Here, the band-diagonal coupling to the phonon bath will lead to so-called *pure dephasing*, i.e. a destruction of the phase coherence of the bare initial two-level systems polarization $p = \langle \hat{a}_v^\dagger \hat{a}_c \rangle$ without relaxation of the excited state occupation. Consider a QD that is excited by a delta-like laser pulse at time $t_0 = 0$. Figure 4 shows how phonons induce an ultra-fast temperature-dependent decay of the polarization on

[4] Before going into an in-depth discussion of the phenomenon a few words concerning the ambiguous term *coherence* might be in order. On one hand it stands for the electronic coherence/polarization between the two QD levels v, c (later also a photon-assisted coherence), which is at least partially lost when interacting with the phonons of the solid-state environment. On the other hand the term *coherent* describes the nature/statistics of the cavity photon field (in contrast to, e.g. a Fock number state). When the electronic system of the QD is strongly coupled to such a *coherent* photon field the *coherent* effect of collapse and revival can arise, where an excitation transfer between the cavity photon number and the electronic occupation (*not* coherence!) of the QD occurs. Although the phonon coupling diagonal in the electronic states leads to a loss of electronic coherence (but not to a loss of the electronic occupation) in the QD, the signatures of the coherent phenomenon of collapse and revival in the photon number persists and can even be stabilized. This is what we refer to when speaking of *phonons supporting coherence effects.*

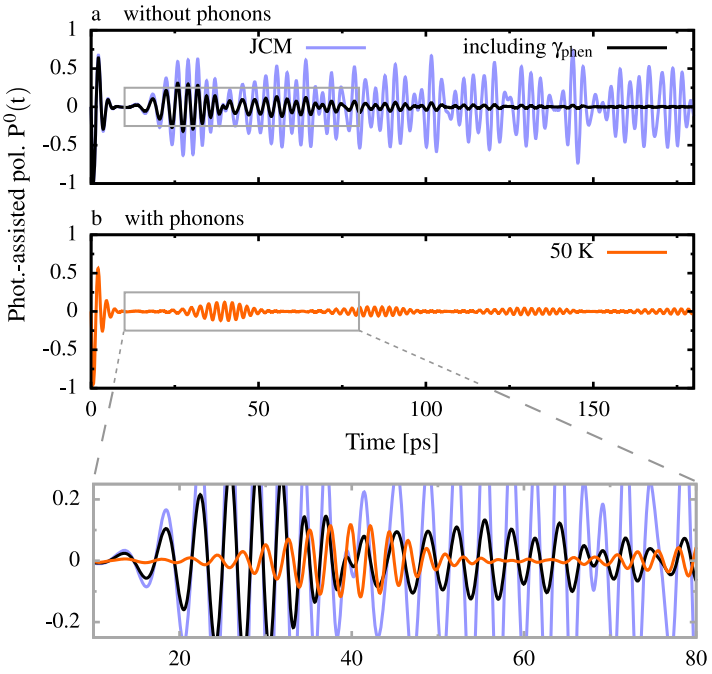

Figure 5. Coherent polarization dynamics. The top panel (a) shows irregular behavior of the JCM solution (blue) without phonons. For comparison the dynamics including $\gamma_{\text{phen}} = 65\,\mu$eV is shown as a black line on top of the blue (undamped) JCM curve, not leading to many-cycle collapse and revivals. The second panel (b) shows the phonon-induced dephasing of P^0 (orange) and resulting pattern formation. The bottom panel shows in a zoom how a phase shift occurs when phonons are considered.

a picosecond time scale. In contrast to a pure exponential decay, as obtained by introducing a simple T_2-time, the initial dephasing in figure 4(a) reveals the non-Markovian nature of the system–bath coupling [36] by a quadratic decay at $t = 0$ and a clearly non-exponential behavior. Indeed, the memory kernel of the electron–phonon interaction [37, 38] persists for up to 4 ps, independent of the bath temperature, see figure 4(b). When including additional phenomenological decays like κ and γ_{rad} the memory kernel will be altered. For small losses the system can retain its non-Markovian nature, but for κ and γ_{rad} in the range of some tens of μ eV losses will dominate and the dynamics becomes Markovian, see discussion at the end of this paper and figure 6.

Turning back to our cavity-QED model, the same decoherence happens to the photon-assisted polarizations $P^m = \langle \hat{a}_v^\dagger \hat{a}_c \hat{c}^{\dagger m+1} \hat{c}^m \rangle$ via their coupling to the phonon system, see equation (A.3) in the appendix. These coherences P^m are the sources for the QD electron dynamics and, via equation (5), for the photon number N, too. Exemplary, the temporal dynamics for $m = 0$, i.e. the photon-assisted polarization $\langle \hat{a}_v^\dagger \hat{a}_c \hat{c}^\dagger \rangle$, is shown in figure 5.

When no phonons are considered figure 5(a) undamped and, at later times, irregular oscillations (blue line) occur after a first collapse and revival event, continuously driving the photon-assisted electron densities X^m. Next, when only a simple phenomenological dephasing constant of $\gamma_{\text{phen}} = 65\,\mu$eV for the electronic polarization is used [39], resembling

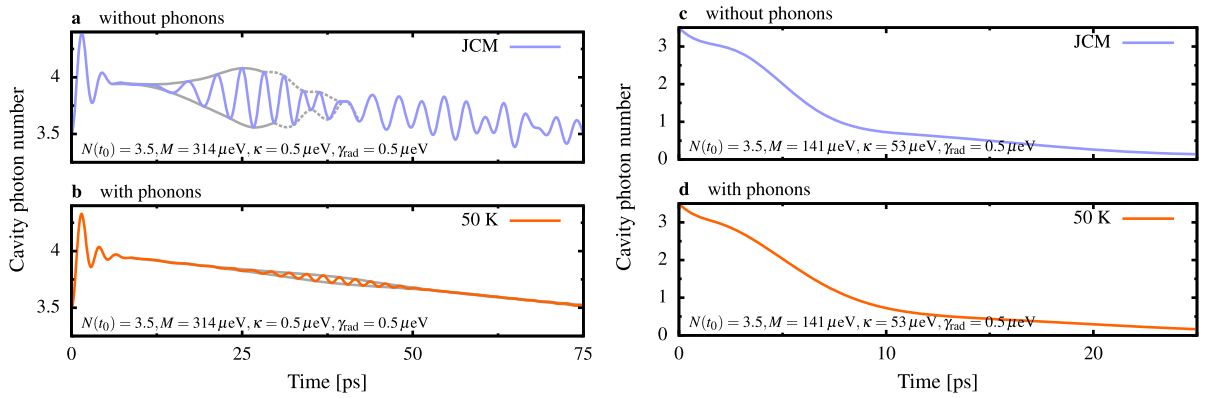

Figure 6. Cavity photon dynamics for different parameter regimes. Panels (a) and (b) show the dynamics for the same electron–photon coupling strength M as used in figure 2, but including a small cavity loss κ and a radiative loss of the QD occupation γ_{rad}. Panels (c) and (d) show the dynamics for a parameter set taken from recent experiments [35].

the Markovian contribution, the oscillation amplitude gets strongly damped, as the blue line in figure 5(a) shows. Since the constant damping affects the coherence at all times any reemerging fluctuations are suppressed.

In stark contrast, figure 5(b) (orange line) shows how the phonons coherent dynamics. Within the first picoseconds a similar damping compared to γ_{phen} occurs. However, due to the temporally finite interaction memory kernel, see figure 4(b), and the continuous driving via the photon field, P^m can revive. Therefore, the initial collapse and revival event is repeated and subsequent revivals can arise, only with a decreased amplitude, since the phonon bath introduces a loss channel in the system.

The zoom below figure 5(b) demonstrates the fundamentally different nature of the full non-Markovian system–bath coupling (orange line), as a clear phase shift in the dynamics occurs, compare with the blue and black line. Each time a coherence builds up, the phonon-induced dephasing will set in, prolonging the revival time, but still allowing for later recovery. Consequently, only the non-Markovian nature of the electron–phonon coupling allows the collapse and revival phenomena to persist and a corresponding pattern within the photon density arises.

Under what terms and conditions do we expect to observe this effect? Firstly, our study is valid within a perturbation theory for the phonons and constitutes an approximative method, as noted by comparison of figure 4(b) with the exact *independent Boson model*. However, since we are still within reasonable limits, we believe that exact numerical calculation available [40] in the future may obtain modifications, but retain our key finding of enhanced collapse and revivals. Secondly, in experimental samples further decay channels are present, e.g. radiative and cavity losses, which will lead to an additional damping of the cavity photon number and QD occupation X^0. As undesirable their influence is in terms of experimental realizations, we want to stress that they do not affect the *principle mechanisms* underlying the stabilization of the collapse and revivals. As for many effects in quantum optics, the decisive quantity here is the ratio between M and $\kappa + \gamma_{\mathrm{rad}}$. If the damping is much weaker than the radiative coupling, i.e. $M \gg (\kappa + \gamma_{\mathrm{rad}})$, the stabilization of the collapse and revivals is still observed, see figures 6(a)

and (b). When much higher losses occur, i.e. $M \ll (\kappa + \gamma_{\mathrm{rad}})$, the cavity photon number will be damped to a point where no Rabi oscillations are observable let alone collapse and revivals, see figures 6(c) and (d). Current semiconductor cQED technology would need a substantial improvement to resolve the presented effect as figures 6(c) and (d) show, where the values for M, κ and γ_{rad} are taken from [35]. In particular we predict a considerably large effect in the few photon limit, in contrast to atomic cQED, as long as none of the interaction dominates the dynamics alone. A strong M is always favorable to the observation of collapse and revivals, but not a necessity:

(i) a weaker M can be compensated for by a higher photon number N (under constant phononic properties of the material) or

(ii) if M is reduced and N is kept constant, the range of the phonon coupling in reciprocal space must be adjusted via the geometry of the QD, its material composition, etc.

Surprisingly, a very strong electron–photon coupling will inhibit the phonon-induced regular coherence features, since the electron–bath interaction becomes negligible compared to the electron–photon coupling [40]. Likewise, high mean photon numbers will outrival the effects of the phonon bath, too. However, throughout our simulations we found that the stabilization of collapse and revivals is very robust for a wide range of different parameters and scenarios. Therefore, with improving sample technology in the future, it should constitute a fundamental phenomenon inherent in the cQED of semiconductor-based devices. Within a quantum well–cavity system, for example, a much higher electron–photon coupling strength M can be achieved, while at the same time operating with higher cavity photon numbers [41]. The phenomenon's robustness relies on the complex interplay between the electron–phonon and electron–photon dynamics. This interplay is governed primarily by the photon number N and the spectral density of the phonon modes. It further depends on the coupling strengths, M and $g_{\mathbf{q}}$, and the temperature of the lattice.

Since the crucial electron–phonon coupling and the corresponding dephasing mechanisms depend on the material parameters, the temperature of the bulk and geometry of the QD, semiconductor technology is not only capable of engineering collapse and revivals with predefined, desired properties, but predestined. Investigating quantum optics with QDs might even advance our understanding of energy transfer in more complex situations, e.g. photosynthesis.

To summarize, the influence of a bath of bulk LA phonons on the coherent dynamics of a QD two-level system in the cQED regime was explored. The well-known random oscillations in the electronic occupation and cavity photon density, typical in the atomic JCM for low photon numbers, where altered significantly. Instead, due to LA phonons inducing a non-Markovian dephasing and thus influencing the coherence time, regular collapse and revivals arise and in an ideal (lossless) scenario last for up to 200 ps depending on temperature.

Acknowledgments

We thank S Müller, M Glässl and M V Axt for fruitful discussions of our numerical results. This work was financially supported by the Deutsche Forschungsgemeinschaft within the Sonderforschungsbereich 787 'Nanophotonik'. AC gratefully acknowledges support from the Alexander-von-Humboldt foundation through the Feodor-Lynen program.

Appendix. Methods

A.1. Numerical parameters

Phonon coupling element $|g_{\mathbf{q}}| = |g_{\mathrm{v}}^{\mathbf{q}} - g_{\mathrm{c}}^{\mathbf{q}}|$, where $g_i^{\mathbf{q}} = \sqrt{\frac{\hbar q}{2\rho c V}} D_i \, \mathrm{e}^{-\frac{q^2\hbar}{4m_i\omega_i}}$. Used parameters: photon order $m = 27$, sound velocity of GaAs $c_{\mathrm{s}} = 5110\,\mathrm{m\,s^{-1}}$, deformation potentials $D_{\mathrm{v}} = -4.8\,\mathrm{eV}$, $D_{\mathrm{c}} = -14.6\,\mathrm{eV}$, effective masses: $m_{\mathrm{c}} = 0.067$, $m_{\mathrm{v}} = 0.45$, confinement energies $\hbar\omega_{\mathrm{c}} = 0.030\,\mathrm{eV}$, $\hbar\omega_{\mathrm{v}} = 0.024\,\mathrm{eV}$ and mass density of GaAs $\rho = 5370\,\mathrm{kg\,m^{-3}}$.

A.2. Dynamics

The general set of coupled equations that determine the electron dynamics and through equation (5) of the paper the photon dynamics as well, are obtained via a method of induction [42], when using the complete Hamiltonian $\hat{H} = \hat{H}_0 + \hat{H}_{\mathrm{el-t}} + \hat{H}_{\mathrm{el-pn}}$ and equation (1) of the paper:

$$\partial_t G^m = -2m\kappa G^m + 2\gamma_{\mathrm{rad}} X^m + \mathrm{i}M[\hat{P}^{m+1} - (P^{m+1})^* + mP^{m-1} - m(P^{m-1})^*], \tag{A.1}$$

$$\partial_t X^m = -(2m\kappa + 2\gamma_{\mathrm{rad}}) X^m - \mathrm{i}M P^{m+1} + \mathrm{i}M (P^{m+1})^*, \tag{A.2}$$

$$\begin{aligned}\partial_t P^m = {} & -\mathrm{i}(\Delta - \mathrm{i}(2m+1)\kappa - \mathrm{i}\gamma_{\mathrm{rad}} - \mathrm{i}\gamma_{\mathrm{phen}}) P^m - \mathrm{i}M \left(mX^{m-1} + X^{m+1} - G^{m+1}\right) \\ & - \mathrm{i} \sum_{\mathbf{q}} g_{\mathbf{q}}^* B_+^m(\mathbf{q}) + g_{\mathbf{q}} B_-^m(\mathbf{q}).\end{aligned} \tag{A.3}$$

The (photon-assisted) ground state density $G^m = \langle \hat{a}_{\mathrm{v}}^\dagger \hat{a}_{\mathrm{v}} \hat{c}^{\dagger m} \hat{c}^m \rangle$ is solely driven by the photon-assisted polarization $P^m = \langle \hat{a}_{\mathrm{v}}^\dagger \hat{a}_{\mathrm{c}} \hat{c}^{\dagger m+1} \hat{c}^m \rangle$ via the electron–photon coupling, as is the excited state density $X^m = \langle \hat{a}_{\mathrm{c}}^\dagger \hat{a}_{\mathrm{c}}^\dagger \hat{c}^{\dagger m} \hat{c}^m \rangle$. The polarization experiences a free rotation due to a possible detuning $\Delta = \omega_{\mathrm{g}} - \omega_0$ of the QD gap energy $\omega_{\mathrm{g}} = \omega_{\mathrm{c}} - \omega_{\mathrm{v}}$ and cavity resonance. A phenomenological cavity loss κ and dipole decay rate γ_{rad} is included, too. We can furthermore account for additional broadenings, observed in experiments, by introducing γ_{phen} [32]. Since κ and γ_{rad} reduce the amplitude of all involved quantities equally, it has no influence on our principle findings of the pronounced collapse and revivals, but much relevance to its experimental observation.

Besides the spontaneous emission of photons ($\propto mX^{m-1}$), crucial for Rabi oscillations, equation (A.3) includes a coupling to phonon–photon-assisted polarizations $B_+^m(\mathbf{q}) = \langle \hat{a}_{\mathrm{v}}^\dagger \hat{a}_{\mathrm{c}} c^{\dagger m+1} c^m \hat{b}_{\mathbf{q}}^\dagger \rangle$ and $B_-^m(\mathbf{q}) = \langle \hat{a}_{\mathrm{v}}^\dagger \hat{a}_{\mathrm{c}} \hat{c}^{\dagger m+1} \hat{c}^m \hat{b}_{\mathbf{q}} \rangle$, too. The dynamics of $B_\pm$ is solved within a Born approximation, where photon-assisted electronic and phononic variables factorize. This yields a closed set in terms of the electron–phonon coupling

$$\partial_t B_+^m(\mathbf{q}) = \mathrm{i}(\Delta - \mathrm{i}(2m+1)\kappa - \mathrm{i}\gamma_{\mathrm{rad}} + \omega_{\mathbf{q}}) B_+^m(\mathbf{q}) - \mathrm{i} g_{\mathbf{q}}^* n_{\mathbf{q}} P^m(\mathbf{q}), \tag{A.4}$$

$$\partial_t B_-^m(\mathbf{q}) = \mathrm{i}(\Delta - \mathrm{i}(2m+1)\kappa - \mathrm{i}\gamma_{\mathrm{rad}} - \omega_{\mathbf{q}}) B_-^m(\mathbf{q}) - \mathrm{i} g_{\mathbf{q}} (n_{\mathbf{q}} + 1) P^m(\mathbf{q}), \tag{A.5}$$

where the mean phonon number $n_{\mathbf{q}} = \langle \hat{b}_{\mathbf{q}}^\dagger \hat{b}_{\mathbf{q}} \rangle$ occurs. For temperatures well below 100 K, as considered here, a second-order Born approximation is well validated to solve the occurring hierarchy problem in the electron–phonon coupling, as can be seen by comparison to exactly

solvable models [43, 44] and experiments. To explore the high-temperature regime, terms beyond second-order must be included or other approaches employed [31].

The phonons of the homogeneous semiconductor material are modeled as a reservoir of harmonic oscillators, which introduces a temperature dependence to the dynamics via the thermal Bose–Einstein distribution function $n_{\mathbf{q}}(T) = (\exp[\hbar\omega_{\mathbf{q}}/k_{\mathrm{B}}T] - 1)^{-1}$. The coupling to the bath will affect the coherent properties of the photon-assisted polarizations P^m over time and lead to a non-Markovian pure dephasing, which cannot be accounted for by introducing the simple, constant dephasing time $T_2 = \gamma_{\mathrm{phen}}^{-1}$ alone.

The complete set of equations (A.1)–(A.5) is, however, not closed in terms of the photon number (m). Therefore, depending on the coupling strength M, a sufficient high order in m is taken into account to reach convergence in the calculations. In the absence of electron–phonon coupling the obtained solution is thus numerically exact and renders the JCM [45].

To have a fair comparison to the JCM, we accounted for the polaron shift in the QD resonance $\Delta_{\mathrm{pol}} = \sum_{\mathbf{q}} |g_{\mathbf{q}}|^2/\omega_{\mathbf{q}}$ by accordingly detuning the cavity, so that both, QD and cavity, are on resonance again. If Δ_{pol} would not have been compensated, a higher Rabi frequency and smaller amplitude would have resulted. We carefully checked our model for detuning effects. Including a strong phenomenological dephasing γ_{phen} allows for a Fourier transformation. A spectral analysis of $P^0(\omega)$ showed that the involved Rabi frequencies in both, the phonon-free JCM and the phonon cases, are essentially in the same spectral range.

A.3. Initial conditions

The initial state of the photon expectation values is derived in dependence of the (given photon statistics and) mean photon number N. The cavity is prepared in a coherent photon state with a mean photon number $N = 3.5$ and thus $\langle \hat{c}^{\dagger m}\hat{c}^m\rangle = \sum_n N^n(\mathrm{e}^N n!)^{-1}\langle n|\hat{c}^{\dagger m}\hat{c}^m|n\rangle = N^m$. Initially the QD is inverted, i.e. $G^m(t_0) = 0.0$ and $X^0(t_0) = 1.0$. The complete density operator ρ considers the electron- ρ^{el} and photon system ρ^{pt}, and reservoirs ρ^{r} (LA phonons and dissipative photon modes). Initially at time t_0, ρ factorizes $\rho(t_0) = \rho^{\mathrm{el}}(t_0) \otimes \rho^{\mathrm{pt}}(t_0) \otimes \rho^{\mathrm{r}}(t_0)$. Consequently, the photon-assisted excited state factorizes $X^m(t_0) = X^0(t_0)N^m$. No coherence is present $P^m(t_0) = B^m_{\pm}(t_0) = 0$. The initial state of the phononic bath is determined by the temperature of the system.

References

[1] Shields A J 2007 Semiconductor quantum light sources *Nature Photon.* **1** 215–23

[2] Michaelis de, Vasconcellos S, Gordon S, Bichler M, Meier T and Zrenner A 2010 Coherent control of a single exciton qubit by optoelectronic manipulation *Nature Photon.* **4** 545–8

[3] Wiersig J *et al* 2009 Direct observation of correlations between individual photon emission events of a microcavity laser *Nature* **460** 245–9

[4] Benson O 2011 Assembly of hybrid photonic architectures from nanophotonic constituents *Nature* **480** 193–9

[5] Ladd T D, Jelezko F, Laflamme R, Nakamura Y, Monroe C and O'Brien J L 2010 Quantum computers *Nature* **464** 45–53

[6] Balandin A A and Nika D L 2012 Phononics in low-dimensional materials *Mater. Today* **15** 266–75

[7] Lanzillotti-Kimura N D, Fainstein A, Balseiro C A and Jusserand B 2007 Phonon engineering with acoustic nanocavities: theoretical considerations on phonon molecules, band structures and acoustic Bloch oscillations *Phys. Rev.* B **75** 024301

[8] Reithmaier J P, Sek G, Löffler A, Hofmann C, Kuhn S, Reitzenstein S, Keldysh L V, Kulakovskii V D, Reinecke T L and Forchel A 2004 Strong coupling in a single quantum dot-semiconductor microcavity system *Nature* **432** 197–200

[9] Cirac J I and Zoller P 1995 Quantum computations with cold trapped ions *Phys. Rev. Lett.* **74** 4091

[10] Hafenbrak R, Ulrich S M, Michler P, Wang L, Rastelli A and Schmidt O G 2007 Triggered polarization-entangled photon pairs from a single quantum dot up to 30 k *New J. Phys.* **9** 315

[11] Carmele A, Milde F, Dachner M-R, Harouni M B, Roknizadeh R, Richter M and Knorr A 2010 Formation dynamics of an entangled photon pair: a temperature-dependent analysis *Phys. Rev.* B **81** 195319
Carmele A and Knorr A 2011 Analytical solution of the quantum-state tomography of the biexciton cascade in semiconductor quantum dots: pure dephasing does not affect entanglement *Phys. Rev.* B **84** 075328

[12] Zoller P *et al* 2005 Quantum information processing and communication *Eur. Phys. J.* D **36** 203–28

[13] Lee H, Cheng Y-C and Fleming G R 2007 Coherence dynamics in photosynthesis: protein protection of excitonic coherence *Science* **316** 1462–5

[14] Mohseni M, Rebentrost P, Lloyd S and Aspuru-Guzik A 2008 Environment-assisted quantum walks in photosynthetic energy transfer *J. Chem. Phys.* **129** 174106

[15] Plenio M B and Huelga S F 2008 Dephasing-assisted transport: quantum networks and biomolecules *New J. Phys.* **10** 113019

[16] Lloyd S 2009 A quantum of natural selection *Nature Phys.* **5** 164–6

[17] Kaer P, Nielsen T R, Lodahl P, Jauho A-P and Mørk J 2010 Non-Markovian model of photon-assisted dephasing by electron–phonon interactions in a coupled quantum-dot–cavity system *Phys. Rev. Lett.* **104** 157401

[18] Ates S, Ulrich S M, Ulhaq A, Reitzenstein S, Löffler A, Höfling S, Forchel A and Michler P 2009 Non-resonant dot–cavity coupling and its potential for resonant single-quantum-dot spectroscopy *Nature Photon.* **3** 724–8

[19] Englund D, Majumdar A, Faraon A, Toishi M, Stoltz N, Petroff P and Vučković J 2010 Resonant excitation of a quantum dot strongly coupled to a photonic crystal nanocavity *Phys. Rev. Lett.* **104** 073904

[20] Hughes S *et al* 2011 Influence of electron–acoustic phonon scattering on off-resonant cavity feeding within a strongly coupled quantum-dot cavity system *Phys. Rev.* B **83** 165313

[21] Hohenester U, Laucht A, Kaniber M, Hauke N, Neumann A, Mohtashami A, Seliger M, Bichler M and Finley J J 2009 Phonon-assisted transitions from quantum dot excitons to cavity photons *Phys. Rev.* B **80** 201311

[22] Ulrich S M, Ates S, Reitzenstein S, Löffler A, Forchel A and Michler P 2011 Dephasing of triplet-sideband optical emission of a resonantly driven InAs/GaAs quantum dot inside a microcavity *Phys. Rev. Lett.* **106** 247402

[23] Kabuss J, Carmele A, Richter M and Knorr A 2011 Microscopic equation-of-motion approach to the multiphonon assisted quantum emission of a semiconductor quantum dot *Phys. Rev.* B **84** 125324

[24] Ota Y, Iwamoto S, Kumagai N and Arakawa Y 2009 Impact of electron–phonon interactions on quantum-dot cavity quantum electrodynamics arXiv:0908.0788

[25] Wilson-Rae I and Imamoğlu A 2002 Quantum dot cavity-QED in the presence of strong electron–phonon interactions *Phys. Rev.* B **65** 235311

[26] Milde F, Knorr A and Hughes S 2008 Role of electron–phonon scattering on the vacuum Rabi splitting of a single quantum dot and a photonic crystal nanocavity *Phys. Rev.* B **78** 035330

[27] Liu B-H, Li L, Huang Y-F, Li C-F, Guo G-C, Laine E-M, Breuer H-P and Piilo J 2011 Experimental control of the transition from Markovian to non-Markovian dynamics of open quantum systems *Nature Phys.* **7** 931–4

[28] Narozhny N B, Sanchez-Mondragon J J and Eberly J H 1981 Coherence versus incoherence: collapse and revival in a simple quantum model *Phys. Rev.* A **23** 236–46

[29] Rempe G, Walther H and Klein N 1987 Observation of quantum collapse and revival in a one-atom maser *Phys. Rev. Lett.* **58** 353–6

[30] Cao H, Jiang S, Machida S, Takiguchi Y and Yamamoto Y 1997 Collapse and revival of exciton–polariton oscillation in a semiconductor microcavity *Appl. Phys. Lett.* **71** 1461–3

[31] Vagov A, Croitoru M D, Glässl M, Axt V M and Kuhn T 2011 Real-time path integrals for quantum dots: quantum dissipative dynamics with superohmic environment coupling *Phys. Rev.* B **83** 094303
[32] Laucht A, Hauke N, Villas-Bôas J M, Hofbauer F, Böhm G, Kaniber M and Finley J J 2009 Dephasing of exciton polaritons in photoexcited InGaAs quantum dots in GaAs nanocavities *Phys. Rev. Lett.* **103** 087405
[33] Majumdar A, Englund D, Bajcsy M and Vučković J 2012 Nonlinear temporal dynamics of a strongly coupled quantum-dot–cavity system *Phys. Rev.* A **85** 033802
[34] Carmichael H J 1999 *Statistical Methods in Quantum Optics 1—Master Equation and Fokker–Planck Equations* (Berlin: Springer)
[35] Volz T, Reinhard A, Winger M, Badolato A, Hennessy K J, Hu E L and Imamoglu A 2012 Ultrafast all-optical switching by single photons *Nature Photon.* **6** 605–9
[36] Madsen K H, Ates S, Lund-Hansen T, Löffler A, Reitzenstein S, Forchel A and Lodahl P 2011 Observation of non-Markovian dynamics of a single quantum dot in a micropillar cavity *Phys. Rev. Lett.* **106** 233601
[37] Vagov A, Croitoru M D, Axt V M, Kuhn T and Peeters F M 2007 Nonmonotonic field dependence of damping and reappearance of Rabi oscillations in quantum dots *Phys. Rev. Lett.* **98** 227403
[38] Kaer P, Nielsen T R, Lodahl P, Jauho A-P and Mørk J 2012 Microscopic theory of phonon-induced effects on semiconductor quantum dot decay dynamics in cavity QED *Phys. Rev.* B **86** 085302
[39] Brossard F S F, Xu X L, Williams D A, Hadjipanayi M, Hugues M, Hopkinson M, Wang X and Taylor R A 2010 Strongly coupled single quantum dot in a photonic crystal waveguide cavity *Appl. Phys. Lett.* **97** 111101
[40] Glässl M, Sörgel L, Vagov A, Croitoru M D, Kuhn T and Axt V M 2012 Interaction of a quantum-dot cavity system with acoustic phonons: stronger light–matter coupling can reduce the visibility of strong coupling effects *Phys. Rev.* B **86** 035319
[41] Khitrova G, Gibbs H M, Kira M, Koch S W and Scherer A 2006 Vacuum Rabi splitting in semiconductors *Nature Phys.* **2** 81–90
[42] Kabuss J, Carmele A, Richter M, Chow W W and Knorr A 2011 Inductive equation of motion approach for a semiconductor QD-QED: coherence induced control of photon-statistics *Phys. Status Solidi* b **248** 872
[43] Förstner J, Weber C, Danckwerts J and Knorr A 2003 Phonon-induced damping of Rabi oscillations in semiconductor quantum dots *Phys. Status Solidi* b **238** 419–22
[44] Förstner J, Weber C, Danckwerts J and Knorr A 2003 Phonon-assisted damping of Rabi oscillations in semiconductor quantum dots *Phys. Rev. Lett.* **91** 127401
[45] Carmele A, Richter M, Chow W W and Knorr A 2010 Antibunching of thermal radiation by a room-temperature phonon bath: a numerically solvable model for a strongly interacting light–matter-reservoir system *Phys. Rev. Lett.* **104** 156801